JACS
JOURNAL OF THE AMERICAN CHEMICAL SOCIETY
Article
pubs.acs.org/JACS

Giant Negative Area Compressibility Tunable in a Soft Porous Framework Material

Weizhao Cai,[†] Andrzej Gładysiak,[†] Michalina Anioła,[†] Vincent J. Smith,[‡] Leonard J. Barbour,*[,‡] and Andrzej Katrusiak*[,†]

[†]Faculty of Chemistry, Adam Mickiewicz University, Umultowska 89b, 61-614 Poznań, Poland
[‡]Department of Chemistry and Polymer Science, University of Stellenbosch, Stellenbosch 7600, South Africa

Supporting Information

ABSTRACT: A soft porous material $[Zn(L)_2(OH)_2]_n$·Guest (where L is 4-(1*H*-naphtho[2,3-*d*]imidazol-1-yl)benzoate, and Guest is water or methanol) exhibits the strongest ever observed negative area compressibility (NAC), an extremely rare property, as at hydrostatic pressure most materials shrink in all directions and few expand in one direction. This is the first NAC reported in metal−organic frameworks (MOFs), and its magnitude, clearly visible and by far the highest of all known materials, can be reversibly tuned by exchanging guests adsorbed from hydrostatic fluids. This counterintuitive strong NAC of $[Zn(L)_2(OH)_2]_n$·Guest arises from the interplay of flexible $[-Zn-O(H)-]_n$ helices with layers of $[-Zn-L-]_4$ quadrangular puckered rings comprising large channel voids. The compression of helices and flattening of puckered rings combine to give a giant piezo-mechanical response, applicable in ultrasensitive sensors and actuators. The extrinsic NAC response to different hydrostatic fluids is due to varied host−guest interactions affecting the mechanical strain within the range permitted by exceptionally high flexibility of the framework.

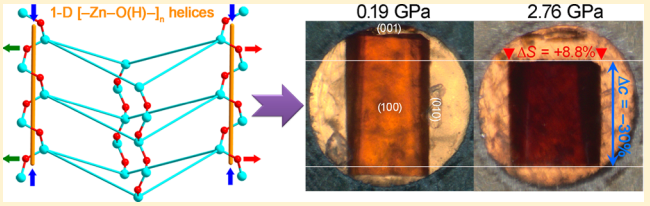

INTRODUCTION

Homogeneous materials capable of deforming to an extent that mimics complicated mechanical devices or biological systems (e.g., muscles) have recently been intensely sought owing to their practically unlimited applications as sensors and actuators.[1] Most materials shrink in all directions under hydrostatic pressure; only few exceptions expand in one direction[2] and even fewer are capable of expanding in two directions when hydrostatically compressed.[3−6] Such expansion in one direction is termed negative linear compressibility (NLC). This effect is rare and usually very small in magnitude. The expansion in two directions of a compressed crystal, known as negative area compressibility (NAC), is much less common (it was evidenced for few structures only) and even weaker in magnitude. It was recently shown that some metal−organic frameworks (MOFs) can expand in one direction at high pressure.[7−9] Here we show that a piezo-responsive MOF $[Zn(L)_2(OH)_2]_n$·Guest (**1·Guest**) deforms so strongly that its record-breaking NAC and colossal positive linear compressibility (PLC) can be appreciated visually (Figure 1). Strong mechanical anisotropy and NLC was recently reported for a handful of crystalline materials.[2] Their expansion along one direction orthogonal to the directions of shrinkage in the hydrostatically compressed structure has been associated with the wine-rack-like geometric motifs in cyanide-bridged coordination polymers,[10−12] metal complexes,[13,14] and molecular crystals.[15,16] NAC, with the direction of strongest compression being perpendicular to the plane of expansion (Figure 1), is the most unusual response to hydrostatic pressure. Such NAC materials could improve, even by an order of magnitude, the sensitivity for piezoelectric response in ferroelectric pressure sensors and might be used as smart elements of devices operating in various environments.[2,5] The counterintuitive NAC effect is extremely rare owing to the complexity of atomic-scale structural motifs counteracting the intuitive compression in all directions. The isothermal NAC coefficient is defined as $\beta_A = -(1/A)(\partial A/\partial p)_T$, the NAC orthogonal plane A of the strain tensor being indicated by the subscript of β. Previously NAC was found in the inorganic oxide NaV_2O_5, for which it was directly measured over the pressure range 4−10 GPa,[3] and possible NAC was theoretically predicted for another layered compound, $TlGaSe_2$.[4] To our knowledge, only two NAC compounds have been confirmed experimentally since 2010: the framework material silver(I) tricyanomethanide, Ag(tcm)[5] and the N−H···N hydrogen-bonded molecular crystal 2-methylbenzimidazole (2MeBzIm)[6] demonstrated new structural features favoring NAC. In Ag(tcm), the weak NAC along the *ac* plane over a narrow pressure range from 0.1 MPa to 0.62 GPa originates from the flattening of corrugated honeycomb-like layers.[5] The giant anisotropic strain and weak NAC of 2MeBzIm above 0.25 GPa are due to "butterfly wing" movements of N−H···N hydrogen-bonded aggregates.[6]

The prominent strain induced by external stimuli (e.g., temperature, pressure, and light) in flexible MOFs has initiated

Received: April 3, 2015
Published: May 6, 2015

DOI: 10.1021/jacs.5b03280
J. Am. Chem. Soc. 2015, 137, 9296−9301

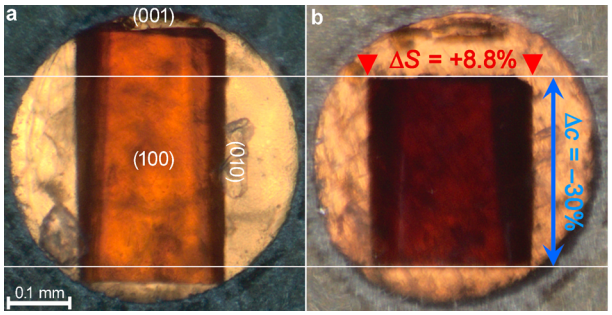

Figure 1. A single crystal of **1·H$_2$O** hydrostatically compressed in isopropanol in the diamond-anvil cell (DAC) chamber. The crystal contracts along direction [001] from (a) 0.441 mm at 0.19 GPa to (b) 0.308 mm at 2.76 GPa. Lines and arrows indicate the relative changes of area ΔS in the expanded surface of face (001) and along the squeezed c axis, respectively.

intense interest in stimulus-responsive functional materials of this type.[17,18] Their mechanical response has been shown to depend on several factors, such as framework flexibility[19] and the nature of adsorbed guests.[20] Intrinsic thermo- and piezo-responsive behavior (e.g., linear/area negative thermal expansion, NTE) has been found in a few wine-rack or quartz-like MOFs,[7,8,21,22] and it was recently shown that this thermal expansion can be finely tuned by exchanging adsorbed guests.[23,24] On the other hand, the anionic contents of one-dimensional (1-D) pores in a hinged framework of [Ag(ethylenediamine)]NO$_3$ strongly enhance the NTE and NLC response, thus violating the inverse relationship rule between linear compression and thermal expansion.[9] We recently established that the unusual area-NTE thermo-mechanical response of the apohost material [Zn(L)$_2$(OH)$_2$]$_n$ (**1**, L = 4-(1*H*-naphtho[2,3-*d*]imidazol-1-yl)benzoate) is tunable by insertion of various alcohol guest molecules into its 1-D channels.[24] The intriguing formation of flexible [−Zn−O(H)−]$_n$ helices in this porous MOF prompted us to investigate the piezo-mechanical response of the material to adsorbed guests over a wide pressure range up to 4.0 GPa. In order to understand the effect of host−guest interactions, the host material **1** with two different guests (Guest = water or methanol) was compressed in three different hydrostatic fluids (silicone oil, methanol−ethanol, and isopropanol). The **1·H$_2$O** samples immersed in isopropanol exhibit giant NAC along the *ab* plane above 1.0 GPa, whereas the NAC of **1·MeOH** in methanol−ethanol (ME, 4:1 by volume) mixture is relatively weak. To our knowledge, this is the first NAC effect observed for a MOF crystal where its piezo-mechanical response is tunable by means of guest exchange.

RESULTS AND DISCUSSION

We have determined the crystal structure of **1·Guest** compressed in three different pressure-transmitting hydrostatic fluids by means of single-crystal X-ray diffraction. All of the crystal structures are isostructural, with the tetragonal space group $I\bar{4}$ persisting and most of the features of the framework preserved.[24] As shown in Figure 2, the framework is composed of strongly puckered quadrangular nets that are interconnected through helical [−Zn−O(H)−]$_n$ chains along the [001] direction. The S_4 symmetry of quadrangular frames implies that all linkers (L) and L−Zn−L angles are equal (Figure 2d). The guest molecules (one per asymmetric unit) in the 1-D channel (~6.0 Å in width) are O−H···O/C−H···O hydrogen-

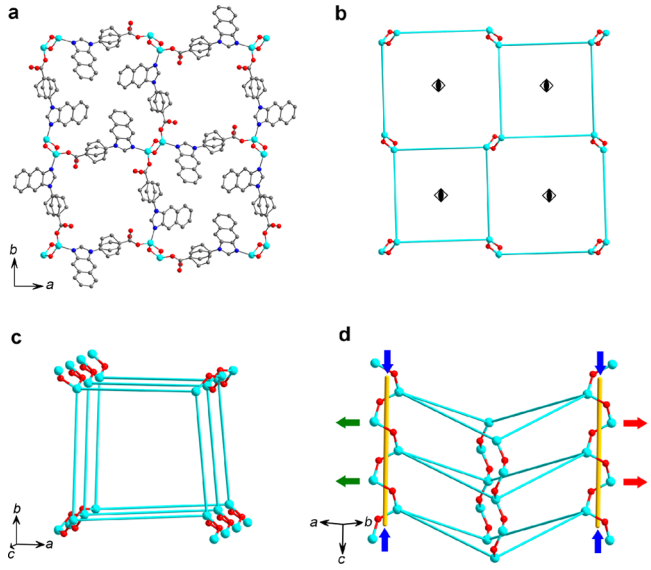

Figure 2. Framework structure of **1·Guest** and its geometric response to hydrostatic pressure. (a) The framework viewed along the c axis. The phenylene rings and oxygen atoms of carboxylate groups are disordered in the organic ligands. (b) The coordination framework simplified into a (4,4)-connected network with [−Zn−O(H)−]$_n$ helices at the corners of large S_4-symmetric quadrangular rings viewed along the 1-D channel pores. (c) The topological structure of one square porous channel viewed along the channel direction. (d) A perspective view of the quadrangular rings connected by the [−Zn−O(H)−]$_n$ helices to form a column along the c axis. The NAC mechanism of **1·Guest** is attributed to the substantial compression of helices along c, coupled to the flattening of puckered quadrangular rings expanding along the *ab* plane. Atoms Zn, O, N, and C are shown as cyan, red, blue, and gray spheres; the cyan sticks represent the −Zn−L−Zn− struts. Hydrogen atoms and guest molecules are omitted for clarity. The red, green, and blue arrows in (d) show the coupling between compression of directions a, b, and c, respectively.

bonded to the L linkers of the host framework (Figures S1 and S2, Supporting Information, SI).

Single crystals of **1·H$_2$O** were immobilized with cotton fibers within the chamber of a modified Merrill−Bassett diamond-anvil cell (DAC), together with several ruby chips for pressure calibration. We first investigated the intrinsic mechanical response of **1·H$_2$O** immersed in silicone oil, because its large molecules prevent any transport into or out of the pores. The initial compression of **1·H$_2$O** is positive along all directions but strongly anisotropic, with the hardest c axis becoming increasingly stiffer and even negatively compressed above 1.0 GPa (Figure 3 and Table S1, SI). This pressure coincides with the limit above which silicone oil becomes pseudohydrostatic.[25] However, the high quality of the **1·H$_2$O** sample up to 2.0 GPa (as judged by microscopic inspection and sharp X-ray reflections) together with the strain observed in the sample (negative along c and positive along b located in equivalent directions parallel to the diamond-anvil culet; and the same along tetragonal a and b, while a was perpendicular to the culet) demonstrate that the effects due to the pseudohydrostatic pressure-transmitting medium are negligible.

The initial volume compression, i.e., below 1.0 GPa, of **1·H$_2$O** in isopropanol is monotonic and consistent with that in silicone oil. Thereafter a discontinuous transition is marked by a considerable drop in volume of −13.0 Å^3 per formula-unit (V/Z). Another more subtle volume discontinuity (V/Z of

DOI: 10.1021/jacs.5b03280
J. Am. Chem. Soc. 2015, 137, 9296−9301

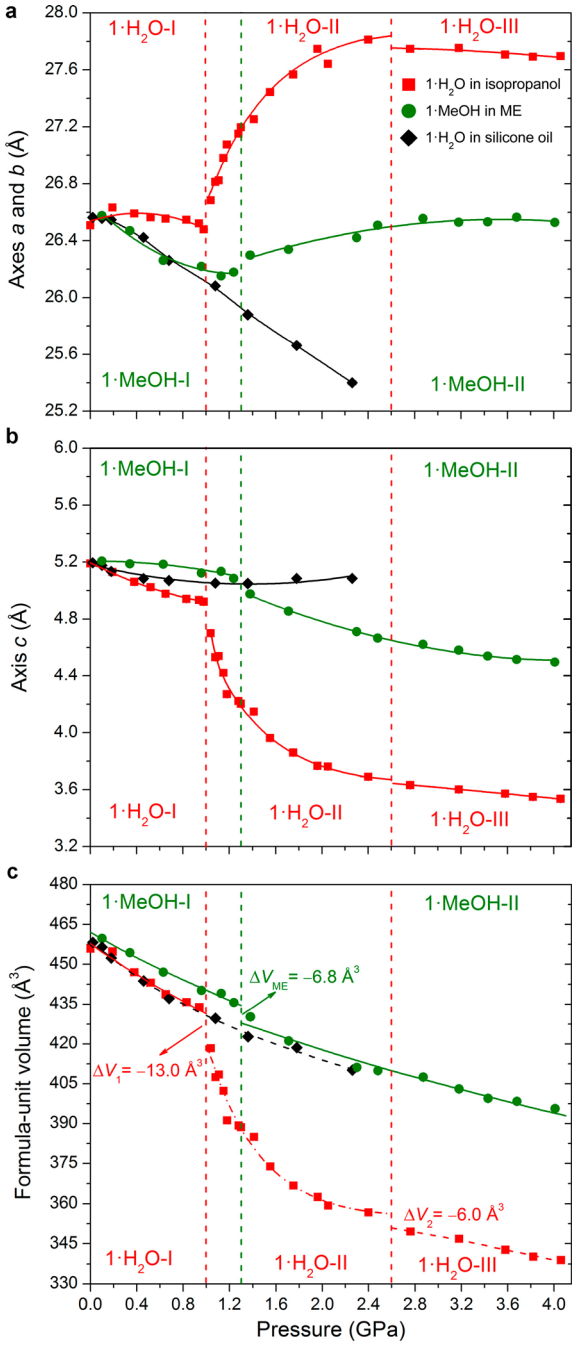

Figure 3. Unit-cell compression of **1·Guest** tuned by three different hydrostatic fluids. Lattice parameters *a* (a) and *c* (b) for silicone oil (black diamonds, **1·H$_2$O**), isopropanol (red squares, **1·H$_2$O**), and the ME mixture (green circles, **1·MeOH**). (c) Formula-unit volume (V/Z) as a function of pressure. Vertical red dashed lines indicate two phase transitions at 1.0 and 2.6 GPa for **1·H$_2$O** compressed in isopropanol; green dashed lines mark the phase transition at 1.3 GPa for **1·MeOH** compressed in the ME mixture. The second- and third-order Birch–Murnaghan equation-of-state fits to the volume (V/Z) data are drawn in solid and dashed lines (the calculated bulk moduli are given in Table S4, SI). The phase II data of **1·H$_2$O** compressed in isopropanol have been fitted with a polynomial curve (dash-dotted line, see SI for discussion).

−6.0 Å^3) occurs at 2.60 GPa. These **1·H$_2$O** phases are termed phase I (**1·H$_2$O-I**, up to 1.0 GPa), phase II (**1·H$_2$O-II** up to 2.60 GPa), and phase III (**1·H$_2$O-III**, above 2.60 GPa). We have established that the two transformations are isostructural with respect to maintaining space-group symmetry and approximate unit-cell dimensions (Figure 3). In our explanation of these transformations the presence of isopropanol in the channel pores of **1·H$_2$O** is crucial. Large molecules of isopropanol enter the framework only in the relatively low-pressure range, up to 0.2 GPa, when the pores are wide enough to allow their diffusion. This intake results in an initial expansion along the *ab* plane and, compared to the reference compression of **1·H$_2$O** in silicone oil, in a small formula-unit volume anomaly (Figure 3c). The transport of isopropanol molecules along the pores is possible, but high pressure narrows the voids and increases steric hindrances, thus hampering their further diffusion. The number of isopropanol molecules distributed stochastically in the bulk of the crystal is relatively small and hence undetectable by X-rays, but large enough to control the crystal compression. Owing to their matched size, the isopropanol molecules block the width contraction of the pores, and the volume compression between 0.2 and 1.0 GPa can only be realized by the *c*-parameter shrinkage. At 1.0 GPa, the accumulated strain is released by the contraction of the structure along *c* coupled to the expansion along *a* and *b* in phase **1·H$_2$O-II**. This mechanism leads to the most pronounced NAC, with *a* and *b* expanding by +4.2% up to 2.60 GPa, while the *c* axis is substantially compressed (by −21.5%, see Figure S3, SI). This giant strain along *c* is clearly visible and allows one to follow the crystal stability regions by observing the changes in crystal shape (Figure 1). On releasing the pressure, **1·H$_2$O-III** transforms back to **1·H$_2$O-II**, and subsequently to phase I; these changes are also easy to discern by observing the crystal shape changes (Figure 1, cf. Figure S4, SI). The compressibility coefficients for the *ab* plane ($\beta_{(001)} = 2\beta_a$) and along the *c* axis (β_c) are −72(6) and +145(9) TPa^{-1}, respectively (Table S2, SI).[26] The NAC magnitude is about an order of magnitude larger than that of Ag(tcm) ($\beta_{(010)}$ = −7.5(8) TPa^{-1})[5] and nearly five times that of the molecular crystal 2MeBzIm ($\beta_{(001)}$ = −15(6) TPa^{-1}).[6] To our knowledge, **1·H$_2$O** is the first MOF crystal exhibiting NAC behavior, the magnitude for which is the highest of all known NAC materials in general.

To substantiate the postulated mechanism of the NAC of **1·H$_2$O** in isopropanol, we compressed a crystal in a pressure-transmitting liquid composed of smaller molecules. Typical porous MOFs with large open pores and extended surfaces allow the transport of small alcohol molecules under high pressure.[27,28] Therefore, a single crystal of **1·H$_2$O** was mounted in the DAC filled with the ME mixture. When pressure was increased to above 0.2 GPa, small cracks appeared on the crystal surface, and at about 0.3 GPa the cracks extended through the entire sample. The subsequent X-ray diffraction measurement showed no single-crystal reflections for the sample. Such destruction of the single crystal compressed in the ME mixture was confirmed for several **1·H$_2$O** samples. It appears that methanol and ethanol molecules are pushed into the pores, and together with water molecules in the pores they destabilize the sample. However, when the **1·H$_2$O** was kept at 0.10 GPa for 7 days prior to increasing pressure and collecting the diffraction data, the sample preserved its high quality as a single crystal. During this period the water molecules in the 1-D pores are exchanged for methanol guests, which could be located in difference-Fourier maps, whereas no signs of ethanol molecules were detected. Thus, a sample of **1·MeOH** was obtained, and this single crystal could be compressed in the ME mixture to over 4.0 GPa. The water-to-methanol exchange is

DOI: 10.1021/jacs.5b03280
J. Am. Chem. Soc. 2015, 137, 9296–9301

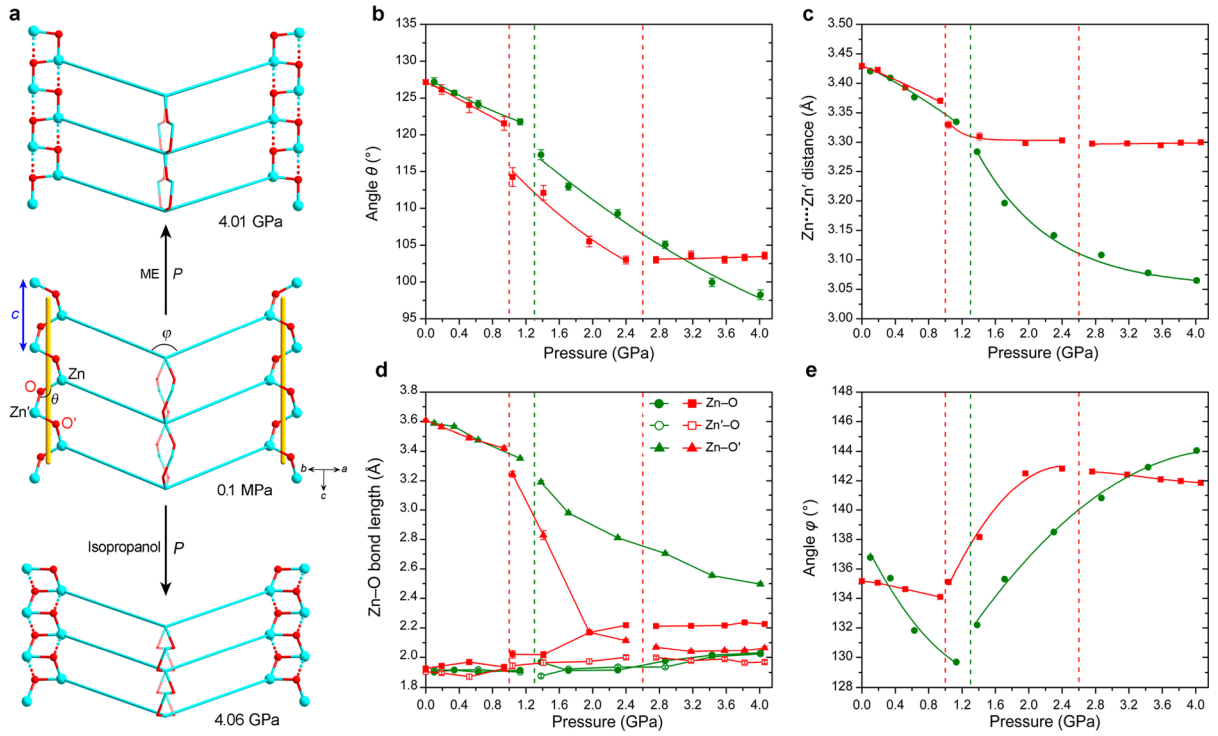

Figure 4. Piezo-mechanical response of **1·Guest** to hydrostatic pressure. (a) The structural change of one square-shaped channel under compression in the ME mixture (top, **1·MeOH**) and in isopropanol (bottom, **1·H_2O**). The stronger compression of $[-Zn-O(H)-]_n$ helix causes a considerable shortening of the *c* axis in isopropanol (for **1·H_2O**), while in the ME mixture the *c* axis is longer and the helix is distorted toward a 1-D zigzag chain (for **1·MeOH**). In the high-pressure structures the nonbonding distances of the $[-Zn-O(H)-]_n$ helix become comparable in length to the bonding distances; these new Zn−O′ coordination bonds are shown in dashed lines. The organic linkers are represented as cyan sticks. The deformation of the helix resembles the compression of a spring, with its pitch equal to the length of lattice parameter *c*. (b) Angle θ (Zn−O−Zn′) versus pressure in phases I, II, and III of **1·H_2O** and phases I and II of **1·MeOH** hydrostatically compressed in isopropanol (red squares) and the ME mixture (green circles), respectively. (c) Compression of Zn···Zn′ distances. (d) Distances Zn−O, Zn′−O, and Zn···/−O′ (the latter transforming into a coordination bond in phase II) (cf. Figure S7, SI). (e) Dihedral angle φ describing the puckering of quadrangular rings. The estimated standard deviations are smaller than the symbols in (c) and (e). The phase transitions in **1·H_2O** and **1·MeOH** are indicated by vertical red and green dashed lines, respectively.

also consistent with the unit-cell volume, which becomes considerably larger than that of **1·H_2O** immersed and compressed either in silicone oil or in isopropanol. This exchange of water by methanol results in only slightly weaker compression of **1·MeOH** than was observed for **1·H_2O** (Figure 3c and Table S4, SI). At 1.30 GPa, **1·MeOH** undergoes an isostructural transformation, marked by a decrease in volume by −6.8 Å^3 per formula unit (Figure 3c). The crystal phases before and after this transformation at 1.30 GPa are denoted as **1·MeOH-I** and **1·MeOH-II**, respectively. The linear compressibility $\beta_a = \beta_b = 13(4)$ TPa^{-1} and $\beta_c = 17(5)$ TPa^{-1} are all positive throughout phase I. Phase **1·MeOH-II** expands along the *ab* plane when compressed, and its NAC coefficient is −4.6(22) TPa^{-1}, more than 15 times smaller than that of phase **1·H_2O-II** in isopropanol (Tables S2 and S3, SI). Between 1.30 and 4.01 GPa, the *a* and *b* axes increase by only 0.90%, while the *c* axis is strongly compressed by 8.6%, i.e., to 91.4% of the initial volume (Figure S3, SI).

It is apparent that the exceptionally strong effect of different hydrostatic fluids is regulated by guests interacting with the bulk of the crystal through its huge extended surface in the channel pores. Silicone oil molecules block the pores at the crystal surface and prevent any transport of guests to and from the crystal. Isopropanol only initially penetrates into the pores, but even such a small amount of it distributed stochastically is capable of reversing the compressibility of the crystal. On the other hand, the smaller methanol molecules exchange with the water guests. High pressure enhances O−H···O and C−H···O interactions and a stoichiometric amount of methanol guests remains in the pores of compressed **1·MeOH**, interacting with the organic linkers. These different host−guest interactions combine with the pressure effects on the highly flexible framework of quadrangular rings $[-Zn-L-]_4$ and helices $[-Zn-O(H)-]_n$.

The compression of **1·H_2O** in silicone oil compared to that of **1·MeOH** in the ME mixture is very similar up to about 1.0 GPa, which corresponds to the pressure range of phase **1·H_2O-I** compressed in isopropanol. In this pressure range the stoichiometric contents of MeOH guests are observed in the increased volume of the crystal (Figure 3) but have little effect on the distortions of the compressed framework. The compression of **1·H_2O** in silicone oil is significantly different from that of phase **1·MeOH-II** (compressed in the ME mixture above 1.3 GPa) and can be associated with the molecular size and interactions of the MeOH guests. They are considerably larger than H_2O guests, and their steric hindrances and interactions counteract the compression of voids along the *ab* plane. The MeOH molecules are smaller than the isopropanol molecules, and consequently their effect on the NAC of the crystal along the *ab* plane is intermediate between those of **1·H_2O** compressed in silicone oil and **1·H_2O** compressed in isopropanol (Figure 3).

DOI: 10.1021/jacs.5b03280
J. Am. Chem. Soc. 2015, 137, 9296−9301

The different piezo-mechanical responses consistently observed for a series of samples originate from the structural changes of compressed **1·Guest** in different hydrostatic fluids. The 2_1-symmetric $[-Zn-O(H)-]_n$ helices extending along the *c* axis are coupled with $\bar{4}$-symmetric puckered quadrangular rings of Zn^{2+} cations and rigid organic linkers (Figure S5, SI). The reduction of dihedral angles φ in the quadrangular rings decreases their lateral dimension and increases the puckering, but most importantly, it strongly affects the channel-void volume (Figures 4 and S6, SI). Angle θ is abruptly reduced and Zn···Zn′ distances shorten upon transition to **1·H_2O-II**. The Zn···Zn′ distance remains virtually constant when the pressure rises above 1.40 GPa, while angle θ decreases throughout the entire phase II region. These transformations result in a considerable contraction of the Zn−O′ contacts, subsequently forming a new coordination bond and hence increasing the Zn coordination number from 4 to 5 (Figure 4d). This gradual process in phase II changes the Zn−O bond pattern from helical in phase I to zigzag ladder in phase III (Figures 4a and S7, SI). Examples of pressure-induced bond rearrangement were observed recently in other MOFs.[29,30] In **1·H_2O** the framework distortions influence the dihedral angle φ, which increases with pressure to compensate for the void volume reduction until reaching the maximum value of 142.83(2)° just before the transformation to phase III (Figure 4e). The ligand lengths and the inner angles L−Zn−L within the puckered rings also increase simultaneously (Figure S8, SI). Most strikingly, this exceptionally flexible structure becomes so stable in phase **1·H_2O-III** that all its structural parameters are practically constant between 2.60 and 4.06 GPa.

The variation of **1·MeOH** helices compressed in the ME mixture is very different: the considerable reduction of angle θ and the Zn···Zn′ distance is coupled to the shortening of the $[-Zn-O(H)-]_n$ helix until 4.01 GPa (Figure 4, also see torsion angle Zn−O−Zn′−O′ plotted versus pressure in Figure S9, SI). These different structural responses of **1·H_2O** and **1·MeOH** suggest that the water and methanol guests differently bound to the organic linker can significantly affect distortions of the framework (Figure S2, SI). In the pressure regions of NAC in both **1·H_2O-II** and **1·MeOH-II**, the reduced pitch of the $[-Zn-O(H)-]_n$ helices is coupled to reduced puckering of the quadrangular $[-Zn-L-]_4$ ring, and so the *c* axis becomes shorter as the *a* and *b* axes become longer with increasing pressure. A similar mechanism was described for modeling the area NTE in a molecular organic crystal (*S*,*S*)-octa-3,5-diyn-2,7-diol, but that case involved the inclination of long organic molecules instead of distortion of quadrangular puckered rings.[31,32]

CONCLUSIONS

1·Guest exhibits the largest known NAC and its magnitude can be controlled by the exchange of adsorbed guest molecules. The crystal strain is affected either by the stoichiometric amount of MeOH guests and by stochastically distributed small amounts of isopropanol, and the NAC magnitude depends on the size of the guest. The host−guest interactions are critical for the piezo-mechanical properties of this material: the proposed mechanism involves small amounts of adsorbed guests stochastically distributed in the channel voids and controlling the deformation of the framework. It is the first soft porous MOF showing NAC in a moderate pressure range. This unique property of **1·Guest** results from its coupled structural features of substantial compression of flexible helices giving rise to the flattening and lateral extension of puckered quadrangular rings $[-Zn-L-]_4$ around the channel pores. This novel structural architecture is highly efficient for generating NAC strain, which has implications for designing other NAC materials. Extraordinary piezo-responsive properties such as that of **1·Guest** are desired for new applications, particularly in second-generation multifunctional pressure sensors, artificial composites, and smart actuators. Such an extent of NAC changing in response to different chemical environments involving guest molecules interacting differently with the voids is a new and unusual mechanical feature, widening the scope for exciting properties of MOFs.

METHODS

Synthesis. Single crystals of **1·MeOH** were prepared by the solvothermal method, as reported previously.[24] $Zn(NO_3)_2{\cdot}4H_2O$ (26.1 mg, 0.1 mmol) and 4-(1*H*-naphtho[2,3-*d*]imidazol-1-yl)benzoic acid (28.8 mg, 0.1 mmol) were dissolved in a mixture of DMF (1.0 mL), methanol (1.0 mL), and H_2O (1.0 mL). The reactants were sonicated for 10 min and placed in a 10 mL Teflon-lined autoclave. The vessel was sealed and heated at 100 °C for 48 h and then cooled slowly to room temperature. Large brown single crystals precipitated. Then the as-prepared **1·MeOH** crystals were dried in an oven at 100 °C for 24 h in order to remove methanol guests. However, we carried out ambient-pressure single-crystal X-ray diffraction measurements before high-pressure experiments and found that water guests were adsorbed from the air by the hydrophilic pores (four water guests per *c*-interval in one porous channel and one water molecule per asymmetric unit); these crystals have been designated as **1·H_2O**.

Variable-Pressure Single-Crystal X-ray Diffraction. High-pressure X-ray diffraction measurements were carried out on an Oxford Diffraction Xcalibur Eos diffractometer, with graphite-monochromated MoKα (λ = 0.71073 Å) radiation. Single crystals of **1·H_2O** were mounted in a modified Merrill−Bassett DAC. Silicone oil, anhydrous isopropanol, and methanol−ethanol mixture (ME, 4:1 by volume) were used as the pressure-transmitting media. Pressure was calibrated with a Photon Control spectrometer by the ruby-fluorescence method with a precision of 0.03 GPa. The high-pressure diffraction data were collected at 9 pressure points for silicone oil (0−2.26 GPa), 27 pressure points for isopropanol (0−4.06 GPa), and 15 points for the ME mixture (0−4.01 GPa).

ASSOCIATED CONTENT

Supporting Information

Detailed experimental procedures, Figures 1−13, Tables 1−13, and CIF files. The Supporting Information is available free of charge on the ACS Publications website at DOI: 10.1021/jacs.5b03280.

AUTHOR INFORMATION

Corresponding Authors

* ljb@sun.ac.za
* katran@amu.edu.pl

Notes

The authors declare no competing financial interest.

ACKNOWLEDGMENTS

W.C., A.G., M.A., and A.K. acknowledge the financial support from the Polish Ministry of Science and Higher Education: Faculty of Chemistry, Adam Mickiewicz University, statutory fund S/P-B/015. L.J.B. and V.J.S. thank the National Research Foundation of South Africa for financial support.

DOI: 10.1021/jacs.5b03280
J. Am. Chem. Soc. 2015, 137, 9296−9301

REFERENCES

(1) Osada, Y.; De Rossi, D. E. *Polymer sensors and actuators*; Springer: Berlin, 2000.
(2) Baughman, R. H.; Stafström, S.; Cui, C.; Dantas, S. O. *Science* **1998**, *279*, 1522.
(3) Loa, I.; Syassen, K.; Kremer, R. K.; Schwarz, U.; Hanfland, M. *Phys. Rev. B* **1999**, *60*, R6945.
(4) Seyidov, M. Y.; Suleymanov, R. A. *J. Appl. Phys.* **2010**, *108*, 063540.
(5) Hodgson, S. A.; Adamson, J.; Hunt, S. J.; Cliffe, M. J.; Cairns, A. B.; Thompson, A. L.; Tucker, M. G.; Funnell, N. P.; Goodwin, A. L. *Chem. Commun.* **2014**, *50*, 5264.
(6) Zieliński, W.; Katrusiak, A. *Cryst. Growth Des.* **2014**, *14*, 4247.
(7) Li, W.; Probert, M. R.; Kosa, M.; Bennett, T. D.; Thirumurugan, A.; Burwood, R. P.; Parinello, M.; Howard, J. A. K.; Cheetham, A. K. *J. Am. Chem. Soc.* **2012**, *134*, 11940.
(8) Ogborn, J. M.; Collings, I. E.; Moggach, S. A.; Thompson, A. L.; Goodwin, A. L. *Chem. Sci.* **2012**, *3*, 3011.
(9) Cai, W.; Katrusiak, A. *Nat. Commun.* **2014**, *5*, 4337.
(10) Goodwin, A. L.; Keen, D. A.; Tucker, M. G. *Proc. Natl. Acad. Sci. U.S.A.* **2008**, *105*, 18708.
(11) Cairns, A. B.; Thompson, A. L.; Tucker, M. G.; Haines, J.; Goodwin, A. L. *J. Am. Chem. Soc.* **2011**, *134*, 4454.
(12) Cairns, A. B.; Catafesta, J.; Levelut, C.; Rouquette, J.; van der Lee, A.; Peters, L.; Thompson, A. L.; Dmitriev, V.; Haines, J.; Goodwin, A. L. *Nat. Mater.* **2013**, *12*, 212.
(13) Shepherd, H. J.; Palamarciuc, T.; Rosa, P.; Guionneau, P.; Molnár, G.; Létard, J.-F.; Bousseksou, A. *Angew. Chem., Int. Ed.* **2012**, *51*, 3910.
(14) Woodall, C. H.; Beavers, C. M.; Christensen, J.; Hatcher, L. E.; Intissar, M.; Parlett, A.; Teat, S. J.; Reber, C.; Raithby, P. R. *Angew. Chem., Int. Ed.* **2013**, *52*, 1.
(15) Fortes, A. D.; Suard, E.; Knight, K. S. *Science* **2011**, *331*, 742.
(16) Cai, W.; He, J.; Li, W.; Katrusiak, A. *J. Mater. Chem. C* **2014**, *2*, 6471.
(17) Schneemann, A.; Bon, V.; Schwedler, I.; Senkovska, I.; Kaskel, S.; Fischer, R. A. *Chem. Soc.Rev.* **2014**, *43*, 6062.
(18) Horike, S.; Shimomura, S.; Kitagawa, S. *Nat. Chem.* **2009**, *1*, 695.
(19) Goodwin, A. L.; Kennedy, B. J.; Kepert, C. J. *J. Am. Chem. Soc.* **2009**, *131*, 6334.
(20) Henke, S.; Li, W.; Cheetham, A. K. *Chem. Sci.* **2014**, *5*, 2392.
(21) Collings, I. E.; Tucker, M. G.; Keen, D. A.; Goodwin, A. L. *CrystEngComm* **2014**, *16*, 3498.
(22) Oritz, A. U.; Boutin, A.; Gagnon, K. J.; Clearfield, A.; Coudert, F.-X. *J. Am. Chem. Soc.* **2014**, *136*, 11540.
(23) Zhou, H.-L.; Lin, R.-B.; He, C.-T.; Zhang, Y.-B.; Feng, N.; Wang, Q.; Deng, F.; Zhang, J.-P.; Chen, X.-M. *Nat. Commun.* **2013**, *4*, 2534.
(24) Grobler, I.; Smith, V. J.; Bhatt, P. M.; Herbert, S. A.; Barbour, L. J. *J. Am. Chem. Soc.* **2013**, *135*, 6411.
(25) Angel, R. J.; Bujak, M.; Zhao, J.; Gatta, G. D.; Jacobsen, S. D. *J. Appl. Crystallogr.* **2007**, *40*, 26.
(26) Cliffe, M. J.; Goodwin, A. L. *J. Appl. Crystallogr.* **2012**, *45*, 1321.
(27) Chapman, K. W.; Halder, G. J.; Chupas, P. J. *J. Am. Chem. Soc.* **2008**, *130*, 10524.
(28) Graham, A. J.; Banu, A.-M.; Duren, T.; Greenaway, A.; McKellar, S. C.; Mowat, J. P. S.; Ward, K.; Wright, P. A.; Moggach, S. A. *J. Am. Chem. Soc.* **2014**, *136*, 8606.
(29) Spencer, E. C.; Kiran, M. S. R. N.; Li, W.; Ramamurty, U.; Ross, N. L.; Cheetham, A. K. *Angew. Chem., Int. Ed.* **2014**, *53*, 5583.
(30) Spencer, E. C.; Angel, R. J.; Ross, N. L.; Hanson, B. E.; Howard, J. A. K. *J. Am. Chem. Soc.* **2009**, *131*, 4022.
(31) Das, D.; Jacobs, T.; Barbour, L. J. *Nat. Mater.* **2010**, *9*, 36.
(32) Goodwin, A. L. *Nat. Mater.* **2010**, *9*, 7.

DOI: 10.1021/jacs.5b03280
J. Am. Chem. Soc. 2015, 137, 9296−9301